Spin accumulation near Fe/GaAs (001) interfaces: The role of semiconductor band structure

Q. O. Hu (□□), E. S. Garlid, P. A. Crowell, and C. J. Palmstrøm

Phys. Rev. B **84**, 085306 — Published 22 August 2011

DOI: 10.1103/PhysRevB.84.085306

Spin accumulation near Fe/GaAs (001) interfaces: the role of semiconductor band structure

Q. O. Hu (胡奇)[1], E. S. Garlid[2], P. A. Crowell[2], and C. J. Palmstrøm[1,3]
[1]*Department of Electrical and Computer Engineering,* [3]*Department of Materials, University of California at Santa Barbara, Santa Barbara, CA 93106*
[2]*School of Physics and Astronomy, University of Minnesota, Minneapolis, MN 55455*

We show that the degenerate region which forms in the vicinity of the Fe/GaAs (001) interface in Schottky tunnel barrier heterostructures plays an important role in spin transport. First, it is a prerequisite for a significant spin current to exist in the absence of an applied bias voltage, which is essential for electrical spin detection. Second, it establishes a well-defined electrochemical potential reservoir which functions as the source of spin currents flowing into the bulk of the semiconductor. A rate equation analysis shows that the optimal thickness of the highly doped GaAs layer at the interface is in the range of 20 to 25 nm for Si dopings of 5×10^{18} cm^{-3}, in reasonable agreement with experiment. Both the sign and magnitude of the spin currents are sensitive to very small changes in interfacial electronic structure, as demonstrated in annealing experiments.

PACS numbers:

One of the important questions in semiconductor spintronics is the extent to which the electronic structure in the vicinity of an interface influences spin accumulation in the bulk of a semiconductor. In the case of spin injection through tunnel barriers, it is widely assumed that the spin current flowing in the bulk of a semiconductor is directly related to the spin polarization of the tunneling current flowing from the ferromagnetic contact. Recent experiments, however, have revealed that the spin accumulation inferred from standard measurements, such as Kerr microscopy or electrical detection, depends strongly on bias conditions.[1–4] We consider the example of epitaxial Fe/GaAs (001) Schottky barriers. Under reverse bias, for which electrons flow from Fe into GaAs, majority spin accumulation is observed, which is expected given the Fe density of states (DOS) near the Fermi energy. Under forward bias voltages of less than 0.1 V, minority spins accumulate underneath the injector, as expected for a system with linear response. At larger forward bias, however, majority spin accumulation is observed, in contrast to expectations as well as observations in metallic lateral spin valves.[5,6] Simple drift-diffusion models of spin transport in the bulk semiconductor describe the data quite well under both forward and reverse bias,[2] and for this reason theoretical work has focused on how electrical spin injection and detection in semiconductor spin devices depend on electronic properties near the ferromagnet/semiconductor interface.[7–11] In this paper, we demonstrate that the degenerate region in the vicinity of the ferromagnet/semiconductor interface plays a critical role in determining the magnitudes of the spin currents that flow in the semiconductor bulk.

The Fe/GaAs heterostructures were grown by molecular beam epitaxy in a system with a base pressure of $< 5 \times 10^{-11}$ torr. The sample structure, from top to bottom, was 10 nm Au/10 nm Al/5 nm Fe/n^+ GaAs (d nm)/2.5 μm n GaAs/500 nm GaAs buffer/GaAs (001) substrate, with the degenerately doped n^+ GaAs layer thickness d being the only variable. For lateral spin transport structures, the GaAs buffer was undoped and the substrate was semi-insulating. A set of companion structures for tunneling spectroscopy measurements were grown on doped buffer layers and highly conductive substrates. The n^+ and n GaAs layers were doped with Si at 4.5×10^{18} cm^{-3} and 6×10^{16} cm^{-3}, respectively. For the complete series of samples, d ranged from 5 nm to 30 nm in increments of 5 nm, and an additional sample was grown with $d = 50$ nm. In addition, a control sample which consisted of a $d = 2$ μm thick n^+ GaAs layer (4.5×10^{18} cm^{-3}) on a conductive GaAs substrate, without the n GaAs layer, was also grown for tunneling transport measurements. Fe films were deposited *in-situ* on As-rich $c(4 \times 4)$ reconstructed surfaces at room temperature. An atomically abrupt interface without any significant interfacial reaction between Fe and GaAs was observed in scanning transmission electron microscopy.[12] Details of the device fabrication process can be found in Ref. 2.

Band diagram simulations of the heterostructures at 20 K were carried out by solving the Poisson and Schrödinger equations in one dimension self-consistently.[13] The Fermi level at the Fe/GaAs interface was set to yield the experimentally determined Schottky barrier height of 0.77 eV.[14] It can be seen from the simulation results in Fig. 1(a) how the shape of the Schottky barrier changes systematically with increasing d. When $d < 15$ nm, the depletion width is larger than d, and a wide barrier is found, for which the tunneling current is expected to be negligible. When d is greater than 15 nm, the barrier becomes significantly thinner (~ 12 nm) near the Fermi energy, and a degenerate region forms in which the Fermi level is in the conduction band. In the range of d of significance for our experiments, the degenerate region is effectively a quantum well (QW), and for this reason we will use QW to refer to the degenerate region henceforth. As noted by Dery and Sham,[7] and discussed further below, the confinement of electrons in this region must be considered when calculating the tunneling DOS relevant for transport. As d increases from 15 nm to

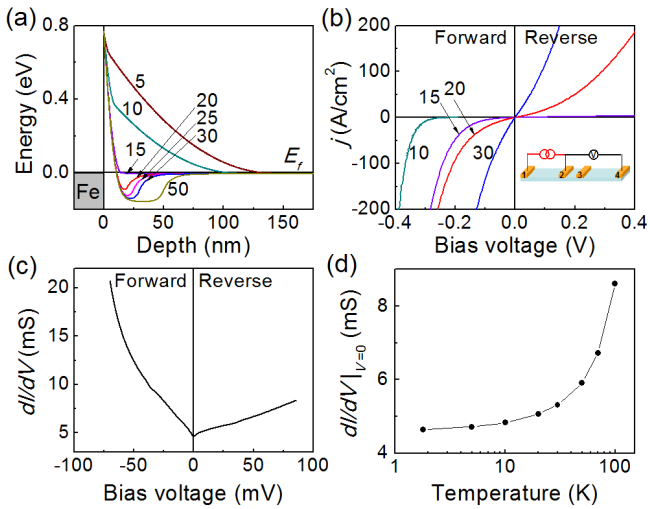

FIG. 1: (Color online) (a) Simulated band diagrams under zero bias at 20 K. The numbers indicate d (in units of nm). (b) Contact $j - V$ characteristics at 15 K. The schematic shows the configuration for the contact $j - V$ measurements. (c) Conductance dI/dV for the $d = 20$ nm sample at 1.8 K. (d) Temperature dependent zero-bias conductance for the $d = 20$ nm sample.

30 nm, there are no significant changes in the barrier profile, but the QW becomes wider and deeper. As d increases above 30 nm, the QW depth remains fixed at approximately 160 meV, but it continues to broaden until the bound states form a continuum.

The current density j measured as a function of bias voltage V at $T = 15$ K for samples with different d's is shown in Fig. 1(b). We will focus on the bias range -0.2 V (forward) $< V < +0.2$ V (reverse), where "forward" refers to electrons tunneling from the semiconductor to the metal. In this regime, j measured for the $d = 5$ nm (not shown) and 10 nm samples is negligible (< 0.06 A/cm^2). A marked change in the character of the $j - V$ curves is observed when $d = 15$ nm, for which the forward bias current (~ 50 A/cm^2 at -0.2 V) exceeds the value expected for a Schottky barrier on n GaAs with a corresponding bulk doping ($n = 6 \times 10^{16}$ cm^{-3}), although j remains small under reverse bias (2 A/cm^2 at $+0.2$ V). When $d > 15$ nm, j exceeds 50 A/cm^2 at $|V| = 0.2$ V in both bias directions, and for these samples it becomes possible to carry out measurements of the differential conductance dI/dV using lock-in techniques. A typical dI/dV measurement at 1.8 K on a sample with $d = 20$ nm is shown in Fig. 1(c), and the zero-bias conductance as a function of temperature for the same sample is shown in Fig. 1(d). Although there is a marked contribution from thermionic emission at higher temperatures, the zero-bias conductance approaches a measurable finite value asymptotically as $T \to 0$.

The transport behavior observed for sufficiently large d is always tunneling-like at low temperatures.[15] A critical fact, however, is the marked change in behavior between $d = 10$ and $d = 20$ nm, over which the onset of tunneling behavior is seen. For larger values of d, the $j - V$ curves become approximately antisymmetric around zero bias, as expected for a heavily doped Schottky tunnel barrier. The excess forward bias current for $d = 15$ nm, however, indicates the presence of filled states in the semiconductor from which electrons can tunnel into the metal. Given the band diagram of Fig. 1(a), this happens only when the Fermi level is above the conduction band minimum in the QW. In other words, the tunneling DOS in forward bias is determined by the DOS in the QW, which is partially filled with electrons. This is in agreement with the more detailed calculations of Song and Dery,[11] who explicitly show that if *only* the tunneling of free electrons from the semiconductor bulk is considered, the tunneling current in the forward bias should be exponentially small compared to reverse bias. The contradiction with the experimental observation is resolved by including the two-dimensional (2D) bound states in the QW as suggested in Refs. 7 and 11. These states contribute significantly to the tunneling current under forward bias.

Detailed tunneling measurements were performed by measuring the contact differential conductance dI/dV and its derivative d^2I/dV^2 as a function of the bias voltage. This method was previously utilized to demonstrate the existence of 2D bound states in a surface accumulation layer at the InAs/oxide interface[16] and the tunneling behavior in spin light-emitting diodes (spin-LED's) with an Fe/AlGaAs Schottky barrier.[15] We focus first on the dispersive features that are observed in all d^2I/dV^2 spectra at reverse bias (positive voltage) in Fig. 2. These features, which are indicated by vertical dashed lines in Fig. 2, show a strong temperature dependence below 20 K and are interpreted to be the longitudinal optical (LO) phonon features in the inelastic tunneling spectrum (at 36 meV for GaAs).[17] We find that the phonon-related features always appear at the same current density for a given heterostructure, and we use

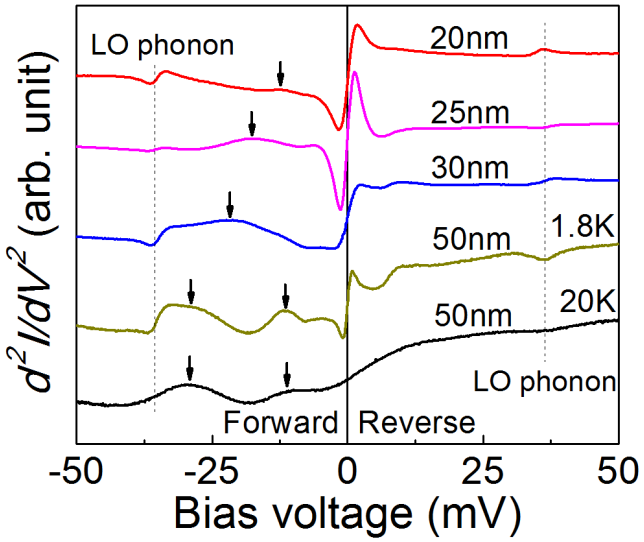

FIG. 2: (Color online) d^2I/dV^2 measured for the samples with $d = 20$, 25, 30, 50 nm at 1.8 K and $d = 50$ nm at 20 K. The arrows indicate the minimum energies of the 2D subbands relative to the Fermi energy of the semiconductor.

this fact to determine the series resistance for each device. The series resistance is then used to determine the actual interfacial voltage shown on the x-axis of Fig. 2. As expected, a corresponding set of dispersive features then appears at the LO phonon energy under forward bias (negative voltage). In addition, a zero-bias anomaly[18] is observed in every sample. Our focus here, however, is on the features indicated by arrows in Fig. 2. These features show a much weaker temperature dependence below 20 K than the phonon and zero-bias anomalies, and they do not appear under reverse bias. As d increases from 20 nm to 30 nm, the peak in d^2I/dV^2 moves towards higher bias voltages, and a second peak emerges for $d = 50$ nm.

Based on these observations, we attribute the additional features observed in d^2I/dV^2 under forward bias to tunneling from bound states in the QW, as originally proposed by Dery and Sham.[7] As the forward bias voltage continuously increases, each time when a bound state rises above the Fermi level in the metal, the tunneling DOS in the QW drops by an amount corresponding to the loss of one bound state. This drop in the tunneling DOS results in a drop in the differential conductance[16,19] and a corresponding extremum in the d^2I/dV^2 spectrum. As the width of the QW increases with d, the number of bound states increases, so that the tunneling DOS becomes effectively three-dimensional.

To determine how the width of the QW in the vicinity of the Schottky barrier affects the spin accumulation in the bulk of the semiconductor, we utilize electrical spin injection and non-local detection in non-local spin valves. This scheme is shown schematically in the inset of Fig. 3(a) and discussed in detail in Ref. 2. The ordinate $V_{\uparrow\downarrow} - V_{\uparrow\uparrow}$ in Fig. 3(a) is the difference in the non-local voltage between the antiparallel and parallel states of the Fe source and detection electrodes (labeled 2 and 3 in the schematic diagram). $V_{\uparrow\downarrow} - V_{\uparrow\uparrow}$ is shown as a function of the interfacial bias voltage at the source electrode. A typical measurement data plot is shown in Fig. 3(b). No signal can be detected in the 5 nm, 10 nm and 50 nm samples. One ubiquitous but confusing observation about the non-local data is that the *sign* for a given bias voltage can be either positive or negative. We will return to the interpretation of this fact below, but for now we consider only the magnitude $|V_{\uparrow\downarrow} - V_{\uparrow\uparrow}|$, as shown in Fig. 4(a). We find that $|V_{\uparrow\downarrow} - V_{\uparrow\uparrow}|$ is extremely sensitive to d. For $d = 15$ nm, $|V_{\uparrow\downarrow} - V_{\uparrow\uparrow}|$ is observed under forward bias (10 μV at -0.4 V), but no signal is observed under reverse bias. At $d = 20$ nm, spin accumulation is observed for both bias polarities, but then the signal decreases and becomes more symmetric with respect to bias as d increases further. This figure illustrates a correlation that has been observed consistently for the many heterostructures fabricated in our group: the devices which show the largest spin accumulation always operate most effectively under forward bias, with very little spin accumulation observable at reverse bias.

The absence of spin accumulation for $d \leq 10$ nm is expected because the depletion depth exceeds the thickness of the highly doped region, causing the tunneling current to be negligibly small for both spin injection and spin detection. The onset of a measurable $|V_{\uparrow\downarrow} - V_{\uparrow\uparrow}|$ at $d = 15$ nm occurs only because of the existence of the QW, which begins to form at this thickness as seen in Fig. 1(a). At this value of d, simulations indicate that carriers remain confined in the QW under forward bias, but no confinement occurs under reverse bias, suppressing the tunneling current and hence the spin accumulation. As d increases, the QW becomes deep enough to provide confinement at both forward and reverse bias voltages. This is particularly important given that the Schottky interface must function

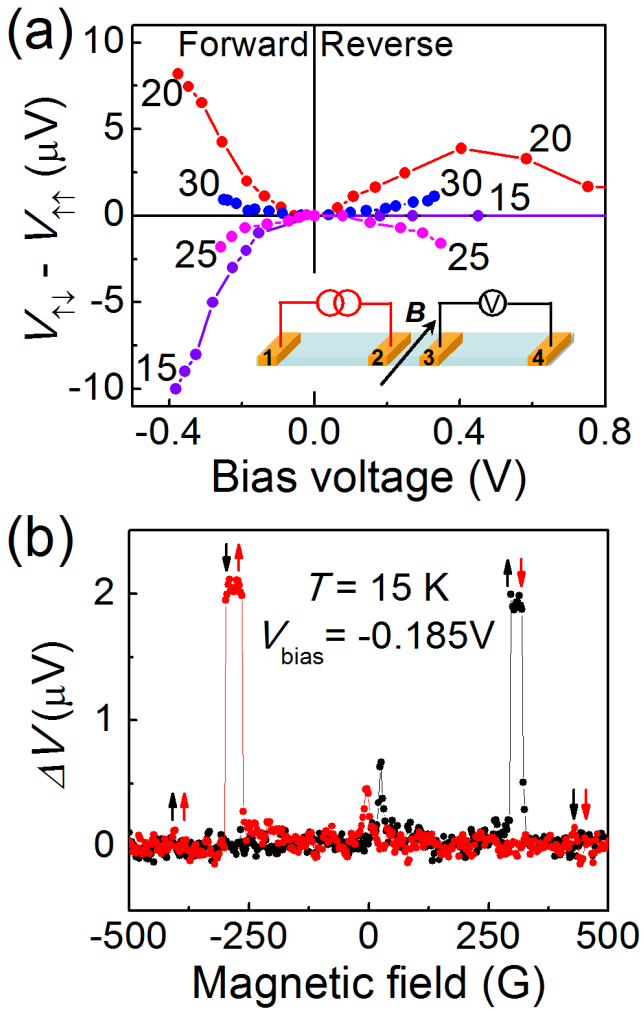

FIG. 3: (Color online) (a) Non-local spin valve voltage $V_{\uparrow\downarrow} - V_{\uparrow\uparrow}$ as a function of injector bias voltage V at 15 K for as-grown samples. The numbers on each curve indicate d in units of nm. The inset is a schematic drawing of the measurement configuration. (b) A typical data set at a forward bias of 0.185 V for a sample with $d = 20$ nm.

as a *spin detector*. In order to ensure chemical equilibrium of spins between the semiconductor and the ferromagnet, a well-defined spin current must flow across the Schottky barrier under zero bias. It is impossible to establish this condition in the absence of the QW, even if a tunnel current flows at the biased injector.

When a bias voltage V is applied across the Schottky barrier, a spin-polarized tunneling current j^σ ($\sigma = \uparrow, \downarrow$) flows into the QW, leading to a spin accumulation $\tilde{n}^\uparrow - \tilde{n}^\downarrow$, where $\tilde{n}^\sigma$ is the spin-dependent areal electron density. The steady state value of $\tilde{n}^\sigma$ is set by the balance of the spin-polarized charge current j^σ and the spins flowing between the semiconductor bulk and the QW in the presence of spin relaxation: $j^\sigma = e\tilde{n}^\sigma(1/\tau_s + 1/\tau_{cap})$, where e is the electric charge, τ_s is the spin relaxation time in the QW, and τ_{cap} is the characteristic time for a spin to be transferred from the QW to the bulk. This argument is similar to that invoked for oxide barriers in Ref. 20, although in that case the intermediate layer was presumed to consist of isolated defects with a long capture time. Based on the measurements of Terauchi *et al.* on heavily doped quantum wells (8×10^{17} cm^{-3}),[21] we expect that τ_s is on the order of tens of psec in the QW. An upper bound of the n^+/n GaAs interface resistance is estimated to be a few hundreds of k$\Omega \cdot \mu$m^2 from the zero-bias conductance, which gives τ_{cap} on the order of 100 psec. Since τ_{cap} is of the same order of magnitude as τ_s, electrons in the QW are spin-polarized. In fact, in the limit of $\Delta\mu^{QW} \ll E_f$, the corresponding electrochemical potential energy splitting in the QW, $\Delta\mu^{QW}$, is

$$\Delta\mu^{QW} = \frac{\tilde{n}^\uparrow - \tilde{n}^\downarrow}{\mathcal{N}^{QW}(E_f)} = \frac{j^\uparrow - j^\downarrow}{e(i \cdot \mathcal{N}^{2D})(1/\tau_s + 1/\tau_{cap})}, \quad (1)$$

where $\mathcal{N}^{QW}(E_f) = i \cdot \mathcal{N}^{2D}$ is the 2D DOS at the Fermi energy E_f in the QW. $\mathcal{N}^{2D} = 2\pi m^*/h^2 = 1.3 \times 10^{13}$ eV^{-1}cm^{-2}

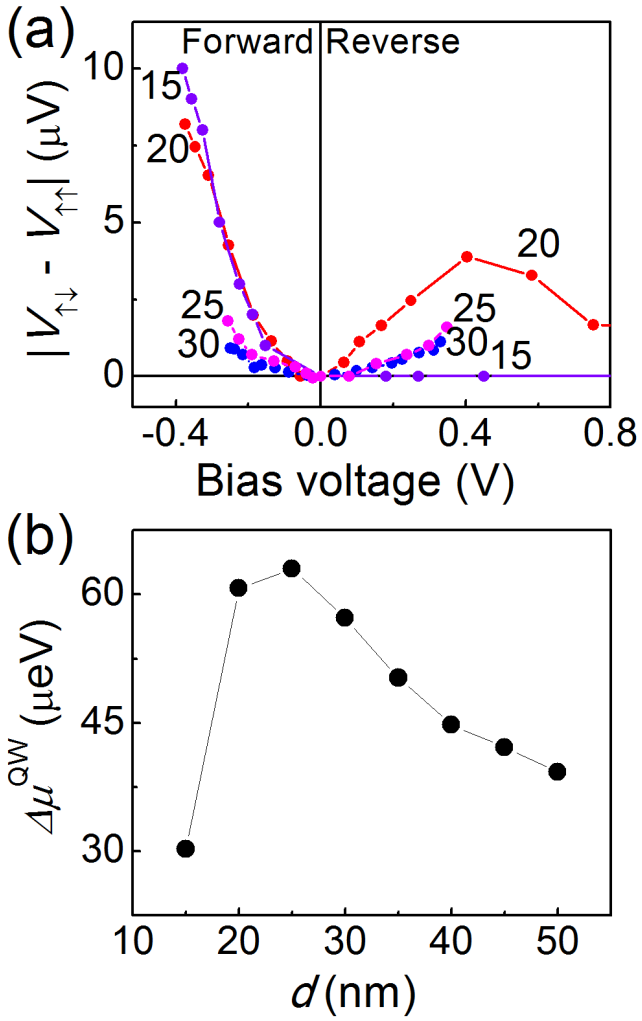

FIG. 4: (Color online) (a) The magnitude of the non-local spin valve voltage $|V_{\uparrow\downarrow} - V_{\uparrow\uparrow}|$ as a function of injector bias voltage V at 15 K for different values of d. (b) The calculated spin accumulation in the QW region $\Delta\mu^{\rm QW}$ as a function of d.

denotes the DOS of one quantized 2D state, where m^* is the effective mass of an electron in GaAs and h is Planck's constant. $i = 1, 2, 3...$ is the number of quantized states below E_f. $\Delta\mu^{\rm QW}$ functions as either the source or sink of a spin current flowing into or from the bulk at the source or detector. We have calculated j^σ between Fe and the QW using the WKB approximation and the barrier profile of Fig. 1(a). Fe is modeled as a simple single-band ferromagnet with Fermi wave-vectors $k_{\rm fm}^{\uparrow} = 1.1$ Å^{-1} and $k_{\rm fm}^{\downarrow} = 0.42$ Å^{-1}.[22] It is found that j^σ calculated in the WKB approximation increases with d initially but saturates after $d = 30$ nm, above which the barrier profile is essentially fixed. The number of filled states in the QW, however, continues to increase with d. As a result, the calculated $\Delta\mu^{\rm QW}$ decreases above $d = 30$ nm, as shown in Fig. 4(b). A similar analysis can be applied to the detector, which is at zero bias. The spin current drawn by the ferromagnet is negligible and has no effect on the d-dependence of the non-local voltage. In practice, $\Delta\mu^{\rm QW}$ is maximized for $d =$ 15-20 nm, very close to the onset of tunneling.

We now discuss the sign and the magnitude of the non-local spin voltage $V_{\uparrow\downarrow} - V_{\uparrow\uparrow}$ upon annealing. The samples were heated in a N_2 atmosphere at 200 °C for 1 hour. Tunneling conductance measurements show that the series resistance and the inferred energy levels of the 2D quantized states do not change upon annealing. The Schottky barrier height increases slightly (for example, from 0.77 to 0.82 eV).[14] The measured $V_{\uparrow\downarrow} - V_{\uparrow\uparrow}$ after annealing is shown in Fig. 5(a). In all cases, significant changes in the spin valve signal are observed relative to the data on unannealed samples shown in Fig. 3(a). The most dramatic effect is a reversal in the sign of the signal in some cases, although there are other changes, such as the disappearance of the sign change under forward bias in the $d = 20$ nm sample (for bias magnitudes less than 0.4 V).

It has previously been established that low-temperature (< 200 °C) annealing enhances the spin injection efficiency

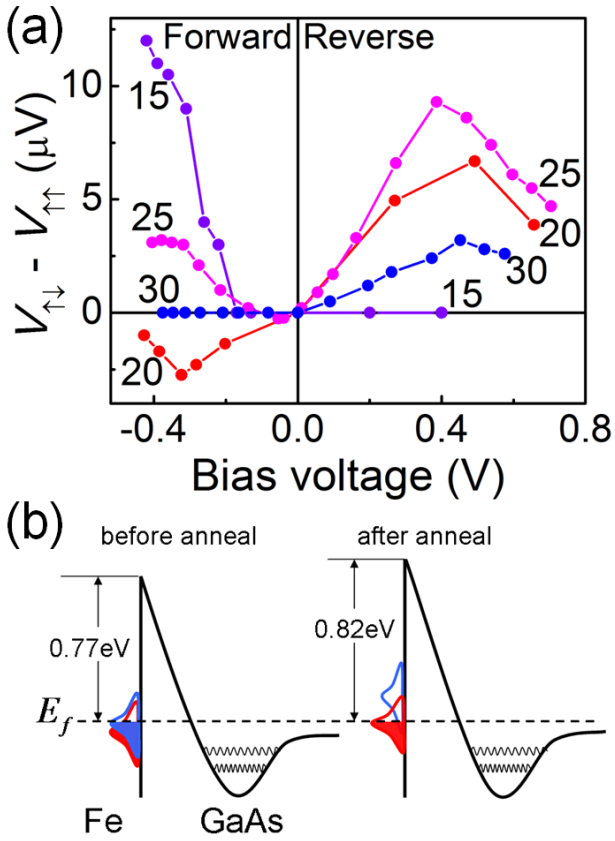

FIG. 5: (Color online) (a) $V_{\uparrow\downarrow} - V_{\uparrow\uparrow}$ as a function of injector bias voltage V at 15 K after anneal. (b) Energy band diagrams of the Schottky barrier interface. For the case shown here, E_f is in the minority-spin band (blue) before anneal and in the majority-spin band (red) after anneal.

of the Fe/GaAs (001) interface as measured in spin-LEDs,[14,23–25] which operate under large reverse bias. In a non-local spin valve, however, the sensitivity of the unbiased detector depends only on the polarization at the Fermi energy E_f. As noted above, the dependence of the spin signal on injector bias voltage clearly indicates a reversal in the sign of the polarization at energies within 0.1 eV of E_f. When considering an *identical* interface functioning as a spin detector, this implies a strong dependence of the magnitude and sign of the detection sensitivity on the exact position of E_f relative to the interfacial band structure. In general, the Schottky barrier height is dominated by interfacial states pinning the Fermi level at metal/GaAs interfaces.[26] The increase in the Schottky barrier height upon annealing is consistent with an increase in the interfacial density of states closer to the valence band, resulting in E_f at the interface being pinned closer to the GaAs valence band. Furthermore, annealing changes not only the interface density of the spin polarized states but also their relative alignment at E_f by either shifting one surface state band relative to another, as shown in Fig. 5(b), or, in a rigid band model, shifting the position of both surface bands relative to the bulk. Notice that the injector bias voltages in our measurements are always large relative to the Fermi level shift, and for this reason the Fermi level shift only impacts the spin-dependent voltage at the detector. This very simple representation ignores any possible changes in the tunneling matrix elements, which are assumed to be independent of spin. Although speculative, the particular situation shown in Fig. 5(b) is consistent with all spin-LED[14,23–25], Kerr microscopy[2,27] and non-local spin valve[2,27] measurements to date, including the recent annealing studies by Salis *et al.*:[4] a significant weight in the minority DOS exists near the Fermi level, and this shifts upwards upon annealing. This increases the degree of spin polarization at and below E_f, which is consistent with both the increase in magnitude of the spin polarization in spin-LEDs as well as the observed enhancement of the non-local spin voltage under reverse bias (the $d = 15$ nm sample remains fully depleted under reverse bias, consistent with an increase in barrier height). The important fact is that the unusual injection bias dependence in the unannealed samples is linked directly to the changes in the sign and magnitude of the detection sensitivity upon annealing. If this behavior can be understood, it points the way to a powerful means to control the spin detection sensitivity by interfacial engineering.

In summary, we have demonstrated how the narrow degenerate region in the vicinity of the ferromagnet/semiconductor interface plays an essential role in spin injection and detection. By systematically varying the Schottky barrier profile while keeping the doping of the bulk semiconductor fixed, the filling of states near the interface modifies the spin accumulation strongly. The interfacial band structure near the Fermi energy changes upon annealing, which modifies the magnitude of the spin accumulation as well as its sign for small bias voltages.

We would like to acknowledge the assistance of K. S. M. Reddy, J. Zhang, Dr. M. K. Chan, Dr. T. Kondo, Dr. A. Kozhanov, and Dr. R. W. Liptak. This work was supported by the ONR MURI program under N00014-06-1-0428, the NSF MRSEC program under DMR-0819885, the NSF IGERT and NNIN programs.

[1] J. Moser, M. Zenger, C. Gerl, D. Schuh, R. Meier, P. Chen, G. Bayreuther, W. Wegscheider, D. Weiss, C.-H. Lai, R.-T. Huang, M. Kosuth, and H. Ebert, Appl. Phys. Lett. **89**, 162106 (2006).

[2] X. Lou, C. Adelmann, S. A. Crooker, E. S. Garlid, J. Zhang, K. S. M. Reddy, S. D. Flexner, C. J. Palmstrøm, and P. A. Crowell, Nature Physics **3**, 197 (2007).

[3] P. Kotissek, M. Bailleul, M. Sperl, A. Spitzer, D. Schuh, W. Wegscheider, C. H. Back, and G. Bayreuther, Natuer Physics **3**, 872 (2007).

[4] G. Salis, A. Fuhrer, R. R. Schlittler, L. Gross, and S. F. Alvarado, Phys. Rev. B **81**, 205323 (2010).

[5] M. Johnson and R. H. Silsbee, Phys. Rev. Lett. **55**, 1790 (1985).

[6] F. J. Jedema, A. T. Filip, and B. J. van Wees, Nature **410**, 345 (2001).

[7] H. Dery and L. J. Sham, Phys. Rev. Lett. **98**, 046602 (2007).

[8] A. N. Chantis, K. D. Belashchenko, D. L. Smith, E. Y. Tsymbal, M. van Schilfgaarde, and R. C. Albers, Phys. Rev. Lett. **99**, 196603 (2007).

[9] D. L. Smith and P. P. Ruden, Phys. Rev. B **78**, 125202 (2008).

[10] A. N. Chantis and D. L. Smith, Phys. Rev. B **78**, 235317 (2008).

[11] Y. Song and H. Dery, Phys. Rev. B **81**, 045321 (2010).

[12] J. M. LeBeau, Q. O. Hu, C. J. Palmstrøm, and S. Stemmer, Appl. Phys. Lett. **93**, 121909 (2008).

[13] G. Snider, 1DPoisson Band Diagram Simulation Program, `http://www.nd.edu/~gsnider/`

[14] C. Adelmann, B. D. Schultz, J. Strand, X. Lou, X. Y. Dong, J. Q. Xie, S. Park, M. R. Fitzsimmons, P. A. Crowell, and C. J. Palmstrøm, in Proceedings of the 16th International Conference on Indium Phosphide and Related Materials, Kagoshima, Japan (IEEE, Piscataway, NJ, 2004), p. 505.

[15] A. T. Hanbicki, O. M. J. van 't Erve, R. Magno, G. Kioseoglou, C. H. Li, B. T. Jonker, G. Itskos, R. Mallory, M. Yasar, and A. Petrou, Appl. Phys. Lett. **82**, 4092 (2003).

[16] D. C. Tsui, Phys. Rev. Lett. **24**, 303 (1970); Phys. Rev. B **4**, 4438 (1971).

[17] J. W. Conley and G. D. Mahan, Phys. Rev. **161**, 681 (1967).

[18] E. L. Wolf, *Principles of Electron Tunneling Spectroscopy* (Oxford University Press, New York, 1989).

[19] D. J. BenDaniel and C. B. Duke, Phys. Rev. **160**, 679 (1967).

[20] M. Tran, H. Jaffrès, C. Deranlot, J.-M. George, A. Fert, A. Miard, and A. Lemaître, Phys. Rev. Lett. **102**, 036601 (2009).

[21] R. Terauchi, Y. Ohno, T. Adachi, A. Sato, F. Matsukura, A. Tackeuchi, and H. Ohno, Jpn. J. Appl. Phys. **38**, 2549 (1999).

[22] M. B. Stearns, J. Magn. Magn. Mat. **5**, 167 (1977).

[23] C. Adelmann, J. Q. Xie, C. J. Palmstrøm, J. Strand, X. Lou, J. Wang, and P. A. Crowell, J. Vac. Sci. Technol. B **23**, 1747 (2005).

[24] T. J. Zega, A. T. Hanbicki, S. C. Erwin, I. Žutić, G. Kioseoglou, C. H. Li, B. T. Jonker, and R. M. Stroud, Phys. Rev. Lett. **96**, 196101 (2006).

[25] B. D. Schultz, N. Marom, D. Naveh, X. Lou, C. Adelmann, J. Strand, P. A. Crowell, L. Kronik, and C. J. Palmstrøm, Phys. Rev. B **80**, R201309 (2009).

[26] E. H. Rhoderick and R. H. Williams, *Metal-Semiconductor Contacts*, 2nd ed. (Oxford University Press, New York, 1988), p. 76.

[27] S. A. Crooker, E. S. Garlid, A. N. Chantis, D. L. Smith, K. S. M. Reddy, Q. O. Hu, T. Kondo, C. J. Palmstrøm, and P. A. Crowell, Phys. Rev. B **80**, R041305 (2009).